Molecular Precursors to Ceramics II[+]

[(Trichlorosilyl)dichloroboryl]ethane: Synthesis and Characterisation by Means of Experiment and Theory

Marcus Gastreich,*[a] Christel M. Marian,[b] Hardy Jüngermann,[c] and Martin Jansen[d]

Dedicated to the memory of Marco Häser

Keywords: TSDE / Ceramics / Theoretical IR-spectroscopy / RI-MP2

A new compound for the molecular synthesis route to high-demand Si/B/N/C ceramics has been found and is described in this work. We report on an elegant "one-pot" synthesis of [(trichlorosilyl)dichloroboryl]ethane (TSDE, $Cl_3Si–CH-[(CH_3)(BCl_2)]$) and its structural characterisation by means of nuclear magnetic resonance and (theoretical and experimental) infra-red spectroscopy. Density functional and Hartree-Fock calculations combined with a perturbational treatment of the electron correlation have been performed. Both methods yield good agreement of theoretical and experimental spectra, with the perturbational approach being slightly superior. In a similar way to the amino compound [(trichlorosilyl)amino]dichloroborane (TADB), TSDE exhibits a planar coordination of the dichloroboryl terminus but tetrahedral neighbourhoods for both carbon and silicon. The electronic structure has been investigated and a $\sigma - n$ order of the frontier orbitals shall be discussed.

Introduction

This paper represents the second part of a series reporting on the synthesis and characterisation of molecular precursors for covalent amorphous Si/B/N/(C) ceramics. As has been shown previously,[2] the so-called *precursor route*, i.e. the way of forming covalent networks from molecular precursors with prebuilt structural units, often leads to most useful high-demand ceramics with outstanding features such as exceptional temperature resistance, corrosion stability and hardness. As examples, we have listed three novel ceramic syntheses and the resulting thermal stabilities of the compounds obtained when using the precursor route shown in Figure 1. The interested reader may find more information on this approach to high-performance ceramics in the literature.[3–5]

In order to understand the structural principles behind these syntheses we have, in this publication, combined experimental and *ab initio* techniques to study the structural properties of [(trichlorosilyl)dichloroboryl]ethane (TSDE) for which a patent has been acquired.[6]

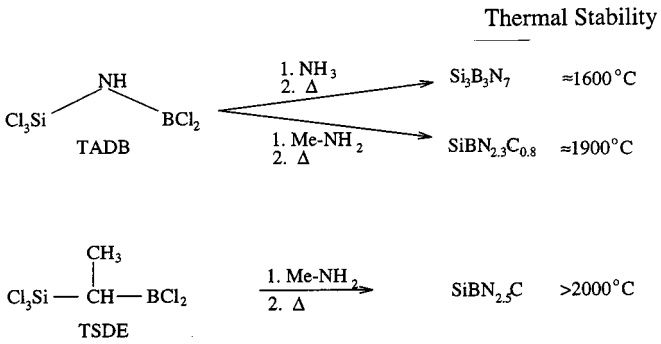

Figure 1. Novel Si/B/N/C-ceramics and their thermal stabilities

Synthesis

0.1 mol of boron trichloride was condensed at −65 °C in a round-bottomed-flask equipped with a dropping funnel and a pressure compensation valve. 0.1 mol of trichlorovinylsilane and 0.1 mol of triethylsilane were mixed and added to the boron trichloride during 15 min. The mixture was stirred for 1h and allowed to warm up to room temperature. The reaction mixture, consisting of the product and triethylchlorosilane, was distilled over a 30 cm Vigreux column. A 64.1% yield of 1-(trichlorosilyl)-1-(dichloroboryl)ethane (TSDE) was obtained at 35–40 °C/12mbar. At room temperature, the product is a colourless liquid which is extremely sensitive to moisture and air.[7]

[+] Part I: Ref.[1]

[a] Institut für Physikalische und Theoretische Chemie Universität Bonn,
Wegelerstr. 12, D-53115 Bonn, Germany
[b] GMD-Forschungszentrum für Informationstechnik GmbH, Schloß Birlinghoven,
D-53754 Sankt Augustin, Germany
[c] Bayer AG, Zentrale Forschung,
D-51368 Leverkusen, Germany
[d] Max-Planck-Institut für Festkörperforschung,
Heisenbergstr. 1, D-70569 Stuttgart, Germany

  1434–1948/99/0101–0075 $ 17.50+.50/0

Characterisation

Experimental Setup

Infra-Red Spectrum: The IR-spectroscopic measurements were conducted using a Fourier transform infrared (FT-IR) spectrometer (model IFS 113v, Bruker Co., Karlsruhe, Germany). The equipment has a modified interferometer by Genzel. Compared to a machine with a Michelson arrangement and the same optical unit dimensions, we obtain double resolution. A globar was used as the light source in the MIR range, and a mercury-cadmium telluride photodetector registered the transmission. No smoothing operators were applied, but a baseline correction was carried out. A liquid sample of neat TSDE was deposited in a cuvette with KBr windows and the spectrum was measured in the absence of water vapor and air at 20 °C.

NMR Spectra: The liquid NMR spectra were recorded on a Bruker AMX 300 spectrometer (Karlsruhe, Germany). The samples had been prepared by mixing neat TSDE with $CDCl_3$ for ^1H as well as for ^{13}C spectroscopy.

Theoretical Methods

Energies and Geometries: Geometry optimisations were carried out with TURBOMOLE v.4.6[8,9] and Gaussian 94.[10] We employed standard relaxation routines based on the Rational-Function or the Quasi-Newton-Raphson models; the initial Hessian matrix was updated by the BFGS algorithm throughout the calculations.[11] At points of vanishing gradient, we determined the matrix of second derivatives of the energy with respect to the nuclear coordinates (Hessian matrix) and computed its eigenvalues to check for imaginary frequencies. Our former investigations were based on molecular hypersurfaces determined on the local density functional level of theory[12] with the Slater exchange- and Vosko-Wilk-Nusair-correlation functionals.[1] These data were reasonable with the exception of hydrogen bond lengths, whose vaues were a bit too long. In the present case, we therefore used the B3LYP[13−15] density functional that employs a three-parameter hybrid functional for the exchange part of the molecular energy and a gradient-corrected functional for the electronic correlation energy. As an alternate correlation treatment to the density functional formalism, we employed the efficient RI-MP2 procedure by Feyereisen, Fitzgerald and Komornicki[16] and implemented by Weigend and Häser[17] to determine both the equilibrium structure and the vibrational spectrum of [trichlorosilyl-(dichloroboryl)]ethane. For the search of the global minimum of the potential energy surface (PES) of TSDE, we have chosen molecular conformers that differed in terms of the relative torsional positions of the BCl_2, $SiCl_3$, and CH_3 groups.

In order to validate the theoretical models with respect to further analysis of the electronic structure, we first calculated the root mean square (rms) deviations of the (scaled) vibrational frequencies for the two different levels of theory. The perturbational correlation treatment was found to be slightly inferior: For B3LYP we determined an rms value of 29 wavenumbers, the perturbational formalism yielded 36 wavenumbers). In any case, we consider the RI-MP2 model advantageous on the basis that one false ordering of frequencies was obtained with the DFT formalism (see below). Thus, subsequent examinations of bonding characteristics etc. will be based on the RI-MP2 geometries, energies and Roothaan-Self Consistent Field (SCF) molecular orbitals for those very geometries.

Basis Sets: The optimisation procedures and energy determinations involved a triple zeta split valence basis set (TZVP) for all methods. It has been taken from the TURBOMOLE v.4.6[8,9] basis set library. This basis set comprises polarisation functions on all atoms including hydrogen. For very small molecules, an RI-MP2 procedure is error-prone due to an insufficient auxiliary basis; we have, however, tested the applicability of the scheme by means of single-point energy calculations on the (full) MP2-level for ammonia, pyruvic acid, CClF(CO), and TSDE itself. Logged errors lie below one millihartree (≈ 0.03 eV); the single-point energy difference (RI- and non-RI-procedures) for the same (RI-MP2-optimised) structure of TSDE only differs by 0.3 millihartrees (≈ 0.008 eV).

Vibrational Spectra: The vibrational spectra have been determined at the corresponding equilibrium geometries by calculating the second derivatives of the electronic energy with respect to the nuclear coordinates; the same basis sets have been employed here. DFT intensities were calculated analytically from the squared derivative of the dipole moment at equilibrium geometry.[18] To calculate RI-MP2 vibrational frequencies, we employed a second derivative numeric procedure that has, amongst others, been linked to the TURBOMOLE-modules. RI-MP2 infra-red intensities have also been numerically determined by calculating the squared dipole moment derivatives with the same grid as for the frequency determination (0.02 bohr ≈ 0.0106 Å). The reliability of the resulting frequencies has, besides the plausible comparison of them with the density functional vibrational values, been tested for compounds that are still easily accessible with the standard MP2-scheme and the software available to us. For these compounds, and with our grid, deviations occur in the regime of only 1−3 wavenumbers compared to analogous analytical calculations. For the intensities, we find deviations of less than one percent. These findings shall be subject to a separate publication.

Results and Discussion

Equilibrium Structure and Stability, Bonding- and Electronic Parameters

Relaxation of the geometrical degrees of freedom of either the staggered or the eclipsed conformations leads to the equilibrium structure represented in Figure 2. We determined slightly different geometric parameters by the different methods. All values and corresponding energies obtained are listed in Table 1.

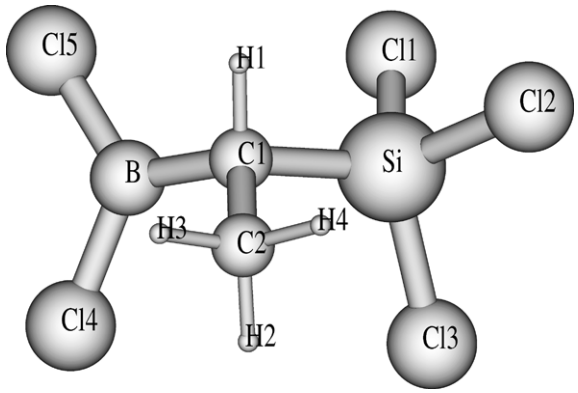

Figure 2. Equilibrium conformation of TSDE

Table 1. Equilibrium geometry data for TSDE for different theoretical models

Coordinate		Theoretical Model RI-MP2//TZVP	B3LYP//TZVP
R [Å]	Cl1−Si	2.046	2.068
	Cl2−Si	2.053	2.075
	Cl3−Si	2.048	2.069
	Si−C1	1.869	1.893
	C1−H1	1.096	1.096
	C1−C2	1.560	1.551
	C2−H2	1.089	1.089
	C2−H4	1.089	1.090
	C2−H3	1.090	1.091
	C1−B	1.560	1.567
	B−Cl4	1.748	1.763
	B−Cl5	1.748	1.764
∠ [°]	Cl1−Si−Cl2	108.39	107.80
	Cl1−Si−Cl3	109.14	108.42
	Cl2−Si−Cl3	108.52	107.97
	Cl1−Si−C1	111.71	111.94
	Cl2−Si−C1	108.73	108.90
	Cl3−Si−C1	110.28	111.66
	Si−C1−H1	103.04	101.99
	Si−C1−C2	109.83	110.34
	Si−C1−B	111.24	112.61
	H1−C1−C2	110.52	109.45
	C1−B−Cl4	120.52	121.48
	C1−B−Cl5	120.59	120.76
	C1−C2−H2	111.28	111.62
	C1−C2−H3	110.25	110.09
	C1−C2−H4	111.16	111.21
	H2−C2−H3	107.52	107.22
	H2−C2−H4	108.44	108.40
	H4−C2−H3	108.05	107.65
	Cl4−B−Cl5	118.89	117.76

The central carbon atom is almost perfectly tetrahedrally connected to a planar BCl_2 group and an $SiCl_3$ group that itself is tetrahedrally coordinated. A C−C distance of 1.560 Å corresponds to a typical single bond length. In addition, the Si−C and B−C bonds lie in the region of typical bond lengths for singly-bonded molecules. The single bond character of all bonds in TSDE is in contrast to the findings in TADB, which exhibits a partially doubly-bonded central pattern with its B−N bond having a length of 1.42 Å.[1]

We found a HOMO-LUMO gap for the closed-shell compound TSDE that amounts to 0.5161 hartrees, i.e. ≈ 13.9 eV. This value remains basically unaltered upon rotating the trichlorosilyl-, methyl-, or dichloroboryl groups as described below.

Graphical representations of the two SCF frontier orbitals are given in Figures 3 and 4.[19] Treating methyl and hydrogen as topologically equivalent, we may consider the plane defined by B−C−Si a mirror plane. The HOMO in this case corresponds to an *a'* molecular orbital with plain σ-type bonding interactions between (a) the central carbon and the boron atom and (b) between C and Si. A nodal plane on C separates these bonding components. This analysis already gives a clue to the low torsional barrier of $SiCl_3$ around the Si−C bond as shall be discussed in the

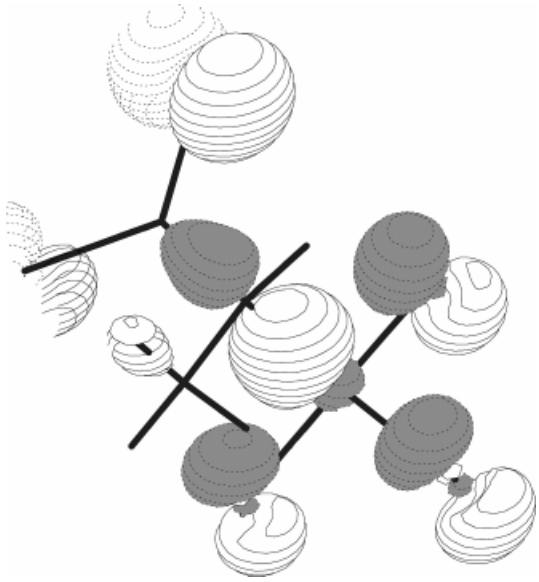

Figure 3. Highest occupied SCF-molecular orbital (HOMO) of TSDE: The BCl_2 group is in the upper left, the $SiCl_3$ group in the lower right corner

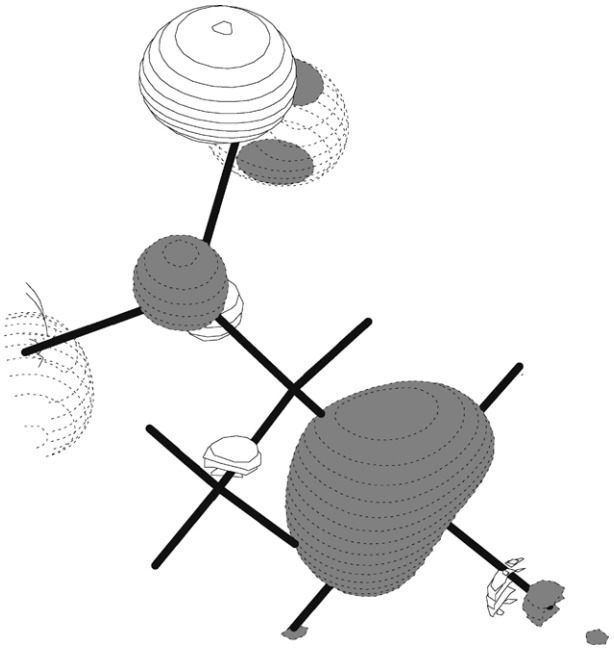

Figure 4. Lowest unoccupied SCF-molecular orbital (LUMO) of TSDE; orientation of the molcule as in Figure 3

section describing the IR spectrum. In addition, the torsion of BCl_2 around the B−C bond should be significantly easier compared to TADB. The HOMO describes the chlorine lone electron pairs as large *p atomic* orbitals that lie almost parallel to the mirror plane, resulting in non-bonded interactions with their neighbouring elements Si and B.

The LUMO, on the other hand, mainly consists of the boron and chlorine *p* atomic orbitals that are perpendicular to the BCl_2 plane. There are three nodal planes with respect to these orbitals: one within the BCl_2 plane, and the two others between B and each Cl. Thus, both B−Cl interactions are anti-bonding, which is, in fact, a very similar situation to that in TADB. The second characteristic constituent of the LUMO is a diffuse silicon atomic orbital with mostly *s* and little *p*-character, the latter being invisible in Figure 4 because of the overlying spacious *s* parts. As we did not include Rydberg or negative ion basis functions[20] in our basis set, we may not judge from this point whether this molecular orbital corresponds to a Rydberg state or not. When exciting electrons into this LUMO, one does not expect this to have a significant influence on the $SiCl_3$ and BCl_2 torsional barriers, as the corresponding interactions are nonbonding. Moreover, we have calculated that a BCl_2 torsion around B−C leaves the characteristics of the frontier orbitals mostly unaltered so that the bond distances will also remain basically the same for such a motion. In summary we can say that the electronic structure of TSDE allows a much higher flexibility when compared to TADB, and the lone pair electrons on all chlorine atoms significantly occupy the HOMO. This may well be a reason for its enhanced functionality as a network-creating agent. The fragment B−C−Si reveals a $\sigma - n$ pattern with respect to HOMO and LUMO.

Infra-Red Spectrum

Figure 5 and the enlarged detail in Figure 6 display the vibrational spectrum obtained experimentally. Embedded within each of these Figures, we have added the line spectrum from theory, and finally Table 2 lists all the data obtained in listed form.

Frequencies have been calculated without anharmonic corrections. Moreover, we have tried to minimise the effects of systematic errors during the calculation of *ab initio* frequencies by scaling the results.[21] The procedure we have applied in this context is widely known as *uniform scaling*[22] and procedes by taking a significant vibrational frequency from the theoretical spectrum and setting this to be equal to the corresponding experimental one. The resulting ratio of frequencies is then used to scale over the entire theoretical spectrum. Thus, we obtain method-specific scaling factors that are given in the header of Table 2. The reference mode was chosen to be the fifth highest in frequency at an experimental value of 1464 wavenumbers: The corresponding signal is in the mid-field region of the spectrum, it can easily be distinguished from the ones at higher wavenumbers, it is sharp, does not show any shoulders, and all theoretical models reproduce the neighbouring signal lower in energy at the experimentally observed distance of approximately ten wavenumbers. The peak chosen in this way appears to be suited best for determining a reasonable scaling factor.

In Figure 5 we have overlayed the full (scaled) RI-MP2 theoretical infra-red line spectrum with the experimental one. For the line spectrum, a ratio of $^{11}B/^{10}B \approx 80{:}20$ has been employed. Assignments from low to high frequencies are easily set up; all calculated values from theory find their

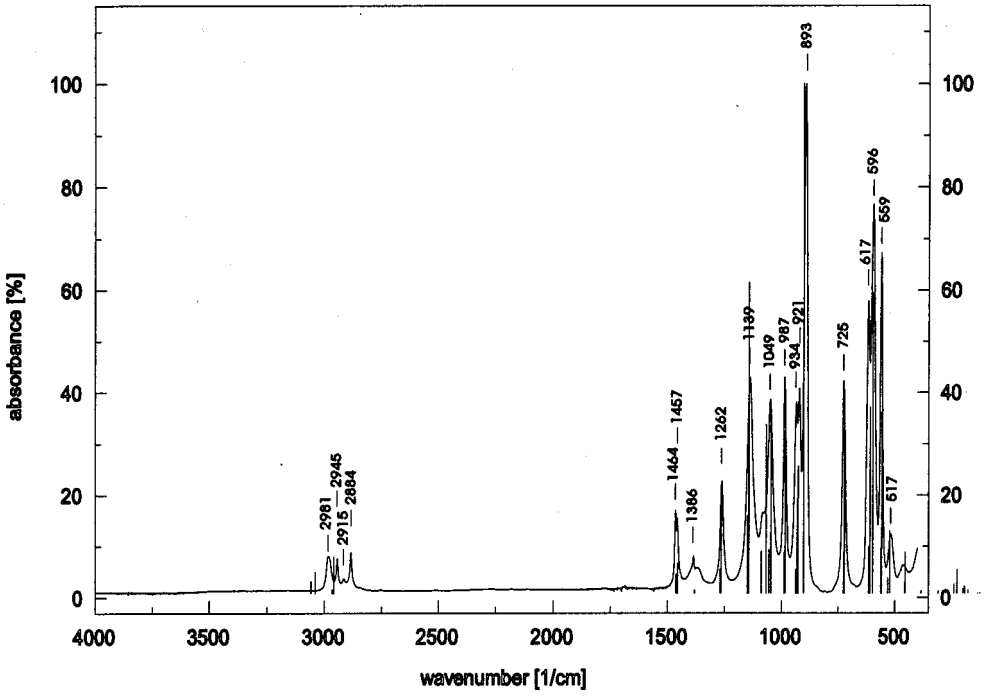

Figure 5. TSDE: Theoretical and experimental IR spectra (Overlay), theory refers to the RI-MP2 level and assumes a $^{11}B/^{10}B$ ratio of 80:20; for reasons of clarity, not all resonances are labelled

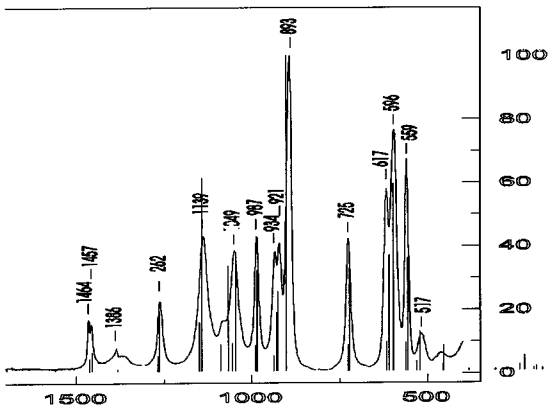

Figure 6. Infra-red spectrum as from Figure 5 − enlargement showing detail of the fingerprint region

experimental counterpart and agreement is particularly good.

Modes 1−12 are basically rocking, bending and wagging motions of the trichlorosilyl- and dichloroboryl-functions, respectively. Mode 13, which we calculate at 383 wavenumbers (scaled RI-MP2), is a combination of a breathing motion of the nuclear frame, accompanied by a slight umbrella-like motion of the methyl group. The experimental spectrum starts with its observation window at around 500 wavenumbers, so the lowest peak in energy at 467 cm^{-1} can clearly be identified with our theoretical value of 454 cm^{-1}, corresponding to mode 14, an umbrella motion of the central carbon atom, combined with symmetric Si−Cl stretching motions and a slight B−Cl stretch vibration. Mode 15 represents the strong pyramidalisation mode of boron, antiphase with Si−C stretches and the $SiCl_3$ umbrella. A theoretical value of 521 cm^{-1} nicely matches an experimental one of 517 cm^{-1}. Still, mode 16 shows a slight out-of-plane (o.o.p.) motion of a boron atom combined with a B−Cl symmetric stretch. Most characteristic for this mode though, are antisymmetric Si−Cl stretch motions and, in this case, theory and experiment agree perfectly (558 vs. 560 cm^{-1}). Mode 17 represents the strong antisymmetric Cl_2Si stretch along with a C−C−Si bending, and a calculated value of 597 wavenumbers finds its experimental counterpart at 596 cm^{-1}. Mode 18, a B−C−Si bending motion, together with an anti-symmetric stretching of the $SiCl_2$ group, shows the same agreement as before: 616 cm^{-1} from the experiment as opposed to 610 cm^{-1} from theory. Mode 19 is a Si−C stretching vibration, exhibiting frequencies of 723 cm^{-1} for the calculated model, and 725 cm^{-1} for the experimental value. This motion is certainly accompanied by a strong in-phase umbrella motion of $SiCl_3$. Mode 20

Table 2. Experimental and theoretical (unscaled and scaled) vibrational frequencies and their relative intensities

Mode	Theory						Experiment		Mode
	DFT Correlation Treatment B3LYP			Perturbation Theoretical Treatment of Correlation RI-MP2					
	ν	ν·0.9676	I[a]	ν	ν·0.9582	I[b]	ν	I	
1	18	17	0	23	22	0			1
2	44	42	0	56	53	0			2
3	80	77	0	86	82	0			3
4	114	111	0	125	120	0			4
5	131	127	0	138	132	0			5
6	169	164	1	181	173	1			6
7	186	180	1	197	189	1			7
8	194	188	0	207	198	1			8
9	205	198	0	232	222	3			9
10	223	215	4	239	229	3			10
11	240	232	1	258	247	1			11
12	307	297	0	320	307	1			12
13	377	365	1	400	383	1			13
14	453	439	9	474	454	8	467	w	14
15	523	506	14	544	521	12	517	m	15
16	549	531	42	583	558	36	559	s	16
17	584	565	54	623	597	61	596	vs	17
18	610	590	21	636	610	38	617	vs	18
19	712	689	29	755	723	33	725	s	19
20	892	863	100	941	902/923	100	893/921	vs/m	20[c]
21	937	906	24	970	930	19	934	s	21
22	1016	983	27	1028	985	33	987	s	22
23	1054	1020	39	1093	1047	35	1049	s	23
24	1106	1070	23	1116	1069	35	1083	s	24
25	1175	1137	41	1192	1143	64	1139	vs	25
26	1304	1262	12	1321	1265	19	1262	s	26
27	1427	1380	1	1444	1384	1	1386	m	27
28	1506	1457	5	1520	1456	6	1457	m	28
29	1513	1464	4	1528	1464	4	1464	m	29
30	3030	2932	1	3091	2962	7	2884	w	30
31	3047	2949	7	3098	2969	1	2915	vw	31
32	3108	3007	4	3176	3043	4	2945	w	32
33	3129	3028	3	3195	3062	2	2981	w	33

[a] 100% = 266 km/mol. − [b] 100% = 244 km/mol. − [c] Refer to text for details.

represents an antisymmetric stretching of BCl_2. We determined an experimental frequency of 893 cm^{-1} which is in accordance with theory (902 cm^{-1}) to within nine wavenumbers. As one can easily tell from looking at a model of atoms moving along this eigenvector, this should be one of the strongest modes in the infra-red spectrum, due to the fact that the dipole moment changes strongly. Indeed, both the density functional and the perturbational calculations determine this vibration as the most intense. Because of its strength we have calculated the corresponding ^{10}B isotopic shift for this mode and found a scaled RI-MP2 value of 923 cm^{-1}. Thus, we conclude that the experimental value of 921 wavenumbers corresponds to a vibration along mode 20 with a ^{10}B nucleus.

Mode 21 basically corresponds to a symmetric stretching vibration of the B−C−Si-fragment that is antisymmetric to a weak BCl_2-vibration of TSDE. A scaled theoretical value of 930 cm^{-1} is nicely reproduced by the experimentally obtained frequency at 934 cm^{-1}. Mode 22 shows the symmetric BCl_2 stretch and some C-B stretching that is antiphase with a wagging motion of the entire methyl group toward the silicon atom. Theory (985 cm^{-1}) and experiment (987 cm^{-1}) match almost perfectly. Mode 23, to which we assign an experimental value of 1049 wavenumbers (theory: 1047 cm^{-1}), shows a B−C−C antisymmetric stretching motion along with a Cl(5)−B stretch. The experimentally recorded shoulder at 1083 wavenumbers correlates with a theoretical resonance at 1069 cm^{-1}, corresponding to mode 24, a strong B−Cl stretch along with a methine-H-C−B bending. Mode 25, which we calculate at 1143 wavenumbers (in satisfactory accordance with the experimental value of 1139) appears as a strong mode in theory and experiment; the corresponding motions are (a) (SiCB) framework stretchings, mainly antisymmetric with respect to B−C and C−Si and (b) an in-plane BCl_2 bending. Mode 26 is mainly an antisymmetric C−C−B stretch. Its vibrational frequency falls into the usual region: 1262 cm^{-1} (experimental), theoretically determined at a scaled value of 1265 cm^{-1}. Mode 27 represents the pure methyl-umbrella motion. We have calculated the corresponding frequency at 1384 cm^{-1}, whereas experiment records it at 1386 cm^{-1}. Modes 28 and 29, at 1457 and 1464 (experimental) or 1456 and 1464 cm^{-1} (theory) respectively, are almost uncoupled scissoring vibrations of the methyl group. The remaining four frequencies in the region of 3000 cm^{-1} certainly belong to C−H stretches. The lowest in frequency (experimental: 2884 vs. theory: 2962) is the symmetric C−H stretch of the methyl group, and mode 31 (experimental: 2915, theory: 2969 cm^{-1}) the methine-H stretch. The density functional calculations reverse the assignment of these frequencies and only by means of a comparison of the calculated intensities (RI-MP2 vs. experiment) can these assignments safely be found. Finally, modes 32 and 33, recorded at 2945 and 2981 cm^{-1} experimentally, are the remaining antisymmetric counterparts of mode 30, the methyl stretches. We calculate these to be at 3043 and 3062 cm^{-1}. As found in most calculations, the agreement slightly deteriorates with higher energies, but the relative positions of the resonances leave assignments unambiguous. Upon turning the trichlorosilyl group through 180° around Si−C and optimising all remaining internal coordinates at the RI-MP2 level, we find a barrier with respect to the minimum of only 9 kJ/mol. Moreover, we have recalculated the vibrational spectrum after this distortion and found deviations of up to 16 wavenumbers (modes 14 and 19). Both these considerations lead us to believe that a thermal excitation should not have influenced characteristics of the experimental infra-red spectrum and that this motion is easily excited at room temperature. Similar considerations apply for the methyl group: A torsion and subsequent relaxation of the remaining internal coordinates yields an energy difference of only 12 kJ/mol above the minimum. The vibrational frequencies deviate at most by 24 cm^{-1} (mode 26) from the equilibrium values. Supported by our considerations for the bond characteristics and the frontier orbitals (see above), one should expect that, finally, a torsion of the dichloroboryl group requires less energy than in TADB (68 kJ/mol), as we had found a partially doubly bonded boron atom there. Indeed, the RI-MP2 energy difference to the minimum amounts to 38 kJ/mol, so this substituent should only be turning freely at slightly elevated temperatures.

NMR Spectrum

The ^1H-NMR spectrum (Figure 7) reveals two signals belonging to the methyl and methine groups of the precursor. The protons of the methyl group are chemically equivalent but the signal at $\delta = 1.48$ is split into a doublet because of the presence of the adjacent methine proton. Analogously, the signal of the methine proton is split into a quartet and is shifted to $\delta = 2.22$.

The signals in the ^{13}C-NMR spectrum (Figure 8) can easily be assigned to the relevant groups: The multiplet in the region of $\delta \approx 78$ belongs to solvent resonances. The methyl group produces a sharp peak at $\delta = 11.93$ whereas the resonance of the methine group is broad and flat and is shifted

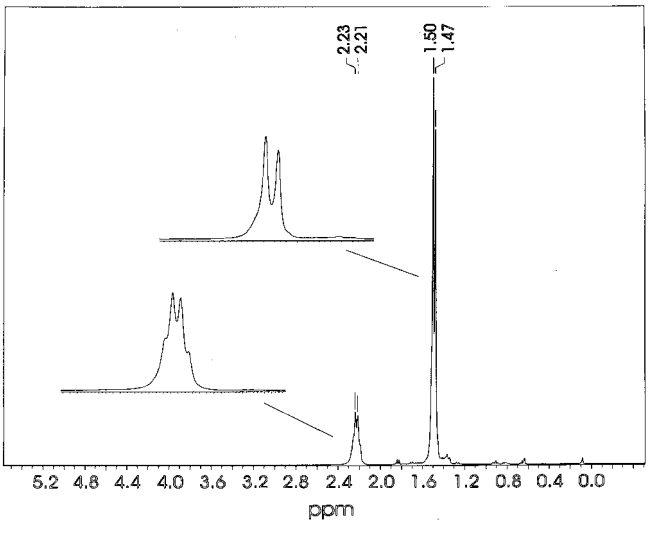

Figure 7. ^1H-NMR spectrum of TSDE

to approximately δ = 34.6. The shape of the latter signal is caused by the interaction of the ^{13}C nuclear spin (I = 1/2) with the quadrupole of the neighbouring ^{11}B (spin 3/2). Table 3 displays results of all NMR experiments conducted (^{1}H, ^{13}C, ^{29}Si, and ^{11}B).

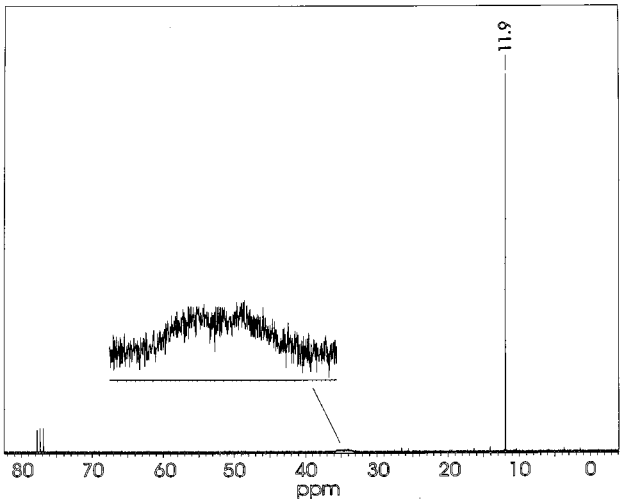

Figure 8. ^{13}C-NMR spectrum of TSDE

Table 3. NMR chemical shifts recorded for TSDE

Nucleus	Chemical shift [δ]	Assignment
^{1}H	1.48	CH_3
	2.22	CH
^{13}C	11.9	CH_3
	34.6	CH
^{29}Si	13.2	$SiCl_3$
^{11}B	67.2	BCl_2

Summary

[(Trichlorosilyl)dichloroboryl]ethane, another member of a group of molecular precursors for Si/B/N/(C) ceramics, is easily accessible through a one-pot synthesis employing boron trichloride and a mixture of trichlorovinylsilane and triethylsilane. As is the case for [(trichlorosilyl)-amino]-dichloroborane, its reasonably flexible equilibrium structure consists of a planar BCl_2 group on one side and a tetrahedral $SiCl_3$ group on the other side of the ethyl backbone. All bonds should be treated as ordinary single bonds, and the HOMO-LUMO sσquence is of $o - n$ character when focusing on the B−C−Si fragment. As far as spectroscopy is concerned, the carbon, hydrogen, boron and silicon NMR signals have been listed and are consistent with the structural analysis. Finally, we have found that second-order perturbation theory reproduces the experimental infrared spectrum with high accuracy and have made the assignments accordingly. By numerically deriving analytical RI-MP2 gradients, we are now able to determine Møller-Plesset second-order perturbational infra-red frequencies. The latter values were obtained with high accuracy for compounds that were barely accessible, or even inaccessible, to such treatment before.

Acknowledgments

This work is dedicated to the memory of Marco Häser, a very able young quantum chemist who died on August 23, 1997 − through his major contributions to the TURBOMOLE package, he substantially diminished the computational efforts we have made within this publication. We are indebted to the HLRZ Supercomputing Center in Jülich and the Cologne University Computing Center. One of us (M.G.) would like to thank Dr Stefan Grimme, Bonn, for helpful discussions. Financial support from the German Research Council (DFG) through SFB408 is gratefully acknowledged.

[1] M. Mühlhäuser, M. Gastreich, C. M. Marian, H. Jüngermann, M. Jansen, *J. Phys. Chem.* **1996**, *100*, 16551.
[2] H.-P. Baldus, O. Wagner, M. Jansen, *Mat. Res. Soc. Symp. Proc.* **1992**, *271*, 821.
[3] H.-P. Baldus, M. Jansen, *Angew. Chem. Int. Ed. Engl.* **1997**, *36*, 328.
[4] M. Peuckert, T. Vaahs, M. Brück. *Adv. Mater* **1990**, *2*, 398.
[5] R. Riedel, *Naturwissenschaften* **1995**, *82*, 12.
[6] H. Jüngermann, M. Jansen, Patent DE 19713766, **1997**.
[7] H. Jüngermann, Doctoral thesis, Bonn University, **1997**.
[8] R. Ahlrichs, M. Bär, M. Häser, H. Horn, C. Kölmel, *Chem. Phys. Lett.* **1989**, *162*, 165.
[9] M. Häser, R. Ahlrichs, *J. Comput. Chem.* **1989**, *10*, 104.
[10] M. J. Frisch, G. W. Trucks, H. B. Schlegel, P. M. W. Gill, B. G. Johnson, M. A. Robb, J. R. Cheeseman, T. Keith, G. A. Petersson, J. A. Montgomery, K. Raghavachari, M. A. Al-Laham, V. G. Zakrzewski, J. V. Ortiz, J. B. Foresman, J. Cioslowski, B. B. Stefanov, A. Nanayakkara, M. Challacombe, C. Y. Peng, P. Y. Ayala, W. Chen, M. W. Wong, J. L. Andres, E. S. Replogle, R. Gomperts, R. L. Martin, D. J. Fox, J. S. Binkley, D. J. Defrees, J. Baker, J. P. Stewart, M. Head-Gordon, C. Gonzales, J. A. Pople, *Gaussian 94, Revision B.1.*, Gaussian Inc., Pittsburgh, **1994**.
[11] H. B. Schlegel, in *Modern Electronic Structure Theory* (Ed.: D. R. Yarkony), World Scientific, **1995**, vol 2, p. 459−500.
[12] R. G. Parr, W. Yang, *Density Functional Theory of Atoms and Molecules*, Oxford University Press, Oxford, **1994**.
[13] A. D. Becke, *J. Chem. Phys.* **1993**, *98*, 5648.
[14] C. Lee, W. Yang, R. G. Parr, *Phys. Rev. B.* **1988**, *37*, 785.
[15] B. Miehlich, A. Savin, H. Stoll, H. Preuss, *Chem. Phys. Lett.* **1989**, *157*, 200.
[16] M. Feyereisen, G. Fitzgerald, A. Komornicki, *Chem. Phys. Lett.* **1993**, *208*, 359.
[17] F. Weigend, M. Häser, *Theor. Chem. Acc.* **1997**, *97(1−4)*, 331.
[18] A. Komornicki, R. L. Jaffe, *J. Chem. Phys.* **1979**, *71(5)*, 2150.
[19] G. Schaftenaar, *Molden 3.2.*, CAOS/CAMM Center, **1996**.
[20] T. H. Dunning, Jr., P. J. Hay, in *Modern Theoretical Chemistry*, vd. 3 (Ed.: H. F. Schaefer III), Plenum Press, **1977**, p. 1−27.
[21] P. Pulay, in *Modern Electronic Structure Theory* (Ed.: D. R. Yarkony), vol. 2, World Scientific, **1995**, p. 1191−1240, and references therein.
[22] W. J. Hehre, L. Radom, P. v. R. Schleyer, J. A. Pople, *Ab Initio Molecular Orbital Theory*, John Wiley, **1986**.

Received July 13, 1998
[I98229]